

NGT-80001

Yanya L. Schrau

IN-29-CR

128716  
358.

LUNAR FIBERGLASS:  
PROPERTIES AND PROCESS DESIGN  
1987 REPORT

by

Robert Dalton

and

Todd Nichols

of

Clemson University

(NASA-CR-182580) LUNAR FIBERGLASS:  
PROPERTIES AND PROCESS DESIGN (Clemson  
Univ.) 35 p CSCI 22A

N88-18740

Unclas  
G3/29 0128716

for the

Universities Space Research Association

Submitted

July 29, 1987

CRE 425/625 SPECIALIZED PROCESSING OF CERAMICS

Semester: Spring 1987

Project: Conceptual design of a plant to produce metal-matrix  
fiberglass on the Moon from lunar raw materials

Faculty: Dr. Ted Taylor

Students: Tim Burke  
William Byrd, Jr.  
David Caldwell  
Robert Dalton  
Scot Graddick (TA)  
Birgit Loescher  
Todd Nichols  
Maria Sachon  
Tanya Schnau  
William Stewart  
Ann Turner

## TABLE OF CONTENTS

Course Data . . . . .	i
List of Figures . . . . .	.iii
List of Tables . . . . .	.iii
Abstract . . . . .	1
Introduction . . . . .	2
Glass Formation . . . . .	3
Glass Manufacturing . . . . .	4
Lunar Glasses . . . . .	5
Metal Matrix Composites . . . . .	7
Geology and Site Selection . . . . .	9
Lunar Fiberglass Plant . . . . .	13
Summer Apparatus . . . . .	19
Summer Work . . . . .	21
Conclusion and Recommendations . . . . .	22
Appendix A: Aerial Ropeway Transportation System . . . . .	23
Appendix B: Mirror Operation and Sizing . . . . .	27
Appendix C: Parent Furnaces . . . . .	29
Appendix D: Lunar Furnace Sizing . . . . .	30
References . . . . .	34

## LIST OF FIGURES

Crystallization Curve . . . . .	3
Continuous Fiberglass Process . . . . .	4
Spinnerette Fiberglass Process . . . . .	5
Composite Cross-section . . . . .	7
Simple Binary Phase Diagram . . . . .	8
Fiberglass Production Flowchart . . . . .	13
Lunar Fiberglass Plant . . . . .	14
Preprocessing . . . . .	15
Furnace Optics: Cassegrainian Setup . . . . .	16
Furnace . . . . .	16
Spinnerette . . . . .	17
Spinnerette - Oblique View . . . . .	18
Collection/Coating . . . . .	18
End Products . . . . .	19
Setup for Making Samples . . . . .	20
Aerial Ropeway Components . . . . .	24
Typical Cable Car . . . . .	26
Pochet Furnace . . . . .	29
American Gas Institute Furnace . . . . .	29
Furnace Sizing Parameters . . . . .	30

## LIST OF TABLES

Compositions of Apollo 16 Samples (Weight %) . . . . .	7
Average Composition of Apollo Soils (Weight %) . . . . .	11

## ABSTRACT

This report presents a Clemson University ceramic engineering class design for a lunar fiberglass plant. The properties of glass fibers and metal-matrix composites are examined, then lunar geology is summarized. A raw material and site are selected based on this information. A detailed plant design is presented, and summer experiments to be carried out at Johnson Space Center are reviewed.

## INTRODUCTION

NASA's long-range plans call for a manned Moon base. When people return to the Moon to stay, they will need to build structures. Since the projected costs of transporting materials from Earth to the Moon are tens of thousands of dollars per kilogram, it would be expensive (perhaps prohibitive) to bring these materials from Earth. An obvious solution is to build with locally available materials. In particular, this paper will investigate the suitability of using local materials for making glass-fiber-reinforced metal-matrix composites, hereafter referred to as fiberglass.

## GLASS FORMATION

When certain materials are heated above their melting point, a liquid is formed which becomes more fluid as the temperature increases. A glass is formed when liquid material is cooled below its melting point, becoming more viscous until the liquid forms a noncrystalline solid. The correct thermodynamic reactions must occur in order for crystals not to form. The reaction is a time-temperature dependent transformation (Figure 1). Temperature

### CRYSTALLIZATION CURVE

(Time-Temperature-Transformation Curve)

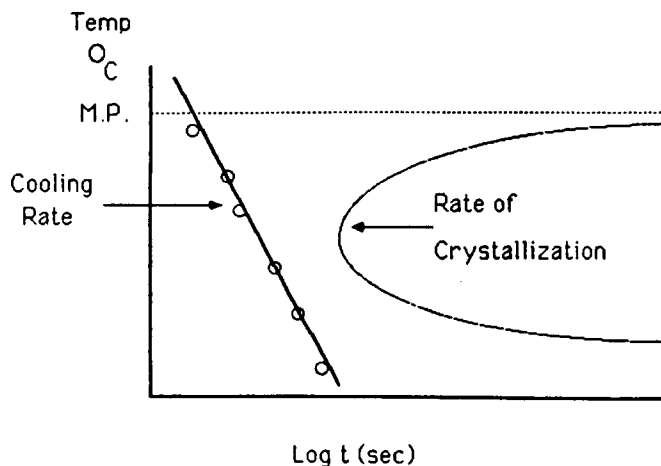


Figure 1

is on the ordinate, and time is on the abscissa. The nose-shaped curve represents the volume fraction of crystal present at the given condition.

In order to form a homogeneous glass the cooling rate of the liquid must cut across the nose-shaped curve, or crystals will nucleate.

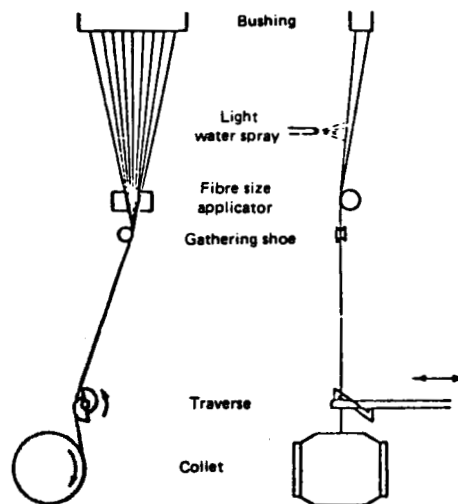
Small additions to the glass system can shift the curve horizontally. Additions of iron and titanium tend to shift the curve to the left, which increases the cooling rate of the glass and makes glass formation difficult.

## GLASS MANUFACTURING

Glass, a noncrystalline solid, can be manufactured into fibers and placed into a matrix to form structural material. The embedding of lunar glass fibers into metals derived from ilmenite processing has good potential for producing structural materials to support a lunar base infrastructure.

Glass fibers are processed two ways on an industrial scale (Doyle, 1979). One produces continuous fibers and the other produces discontinuous fibers. The textile process produces continuous fibers, while the spinnerette process produces discontinuous short fibers.

In the continuous process (Figure 2), glass fibers are drawn



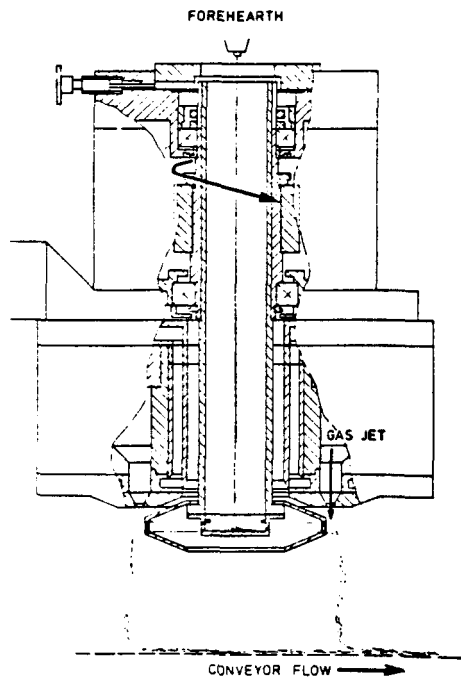
*Fig. 5.26. Schematic representation of mechanical attenuation for the forming of continuous glass fibres. The bushing is fed either with marbles, or directly with liquid glass from a fore-hearth*

Figure 2

from many holes at the bottom of a furnace called bushings and are collected on a spinning spool called a collet. Operation temperatures of the average commercial glass are about 1000° C to



1150° C, which correspond to glass viscosities of approximately 500 to 100 poises. The fiber diameter is dependent on bushing temperature and collet wind speed. This process requires much manual assistance to feed the fiber into the collet when fiber breakage occurs. The process was incorporated into Clemson's experimental apparatus for simplicity and safety.



A typical spinner for the production of glass wool by centrifugal spinning. A stream of glass falls into the rotating spinner, is forced horizontally outwards, and then flame attenuated by gas blast directed towards the conveyor.

The spinnerette process (Figure 3), which produces short discontinuous fibers, uses only a large single bushing. One stream of glass is directed to a spinnerette which contains 4000 small holes in its side. By centrifugal force and gas attenuation the glass is forced out of the basket. The operation viscosity of 1000 poises used in industry lies in a temperature range of 1050° C to 1150° C for commercial glasses. Lunar glass will probably

operate at temperatures above 1150° C and will not use gas attenuation for drawing. The spinnerette process has been incorporated into the glass furnace design because it can be easily automated.

### LUNAR GLASSES

Radiative cooling experiments performed by Ardnt (1977) on typical anorthositic and basaltic lunar glass compositions showed

that basalt must be cooled at a rate of  $30^{\circ}$  K per minute to form nucleation-free glass, while the anorthosite sample did not crystallize at the slowest radiative cooling rates attainable. This may lead one to believe that anorthite would be an ideal glass composition; however, experiments with anorthite (Klein and Uhlmann, 1974) point out that [pure] liquid anorthite held in the range between  $1423^{\circ}$  K and  $1670^{\circ}$  K crystallizes rapidly. This temperature range corresponds to the viscosity needed to produce fiberglass, 500 to 1000 poises. The magnitude of crystallization would make it impossible to produce glass fibers.

In the summer of 1986 at Johnson Space Center, the Clemson group experimented with simulated glass of the average Apollo 16 regolith composition. Glass fibers were pulled over a narrow range from  $1200^{\circ}$  C to  $1250^{\circ}$  C, and nucleation was present. Investigations of Apollo 16 lunar glass (Uhlmann et al., 1977) have shown that sample 67975 (Table 1) is the best glass former. Sample 67975 is higher in  $Al_2O_3$  and  $SiO_2$ , and low in  $TiO_2$ ,  $MgO$ , and  $FeO$ . Glasses of the compositions of Apollo 16 soils 60501 and 61221 were investigated (Ridley et al., 1973). These glasses contained ratios of  $Mg/(Fe+Mg)$  of approximately 0.72, and are thought to be good glass formers. The glass formed from the simulated average Apollo 16 regolith had a ratio of  $Mg/(Fe+Mg)$  of 0.51, and nucleation was present upon formation. The glasses from both investigations were anorthositic in nature. Glass compositions that follow the trends of sample 67975 and soil samples 60501 and 61221 are to be investigated by Clemson this summer at Johnson Space Center.

TABLE 1  
COMPOSITIONS OF APOLLO 16 SAMPLES (WEIGHT %)

Oxide	67975	60501	61221
SiO <sub>2</sub>	44.7	45.24	45.54
Al <sub>2</sub> O <sub>3</sub>	30.4	27.61	27.68
CaO	18.3	15.59	15.73
MgO	1.2	6.40	5.62
FeO	2.5	4.63	4.60
TiO <sub>2</sub>	0.7	0.44	0.42
Mg/Mg+Fe	-	0.73	0.70

#### METAL MATRIX COMPOSITES

Fiber-reinforced composites (Figure 4) are composed of stiff fibers in a plastic matrix. Glass fibers by themselves are very strong, but are also very brittle. When they are embedded in a ductile matrix and the material is stressed, the matrix deforms and distributes some of the stress more evenly throughout the fiber network. A metal-matrix composite, then, has most of the strength of the fibers and most of the toughness of the matrix.

#### Composite Cross-section

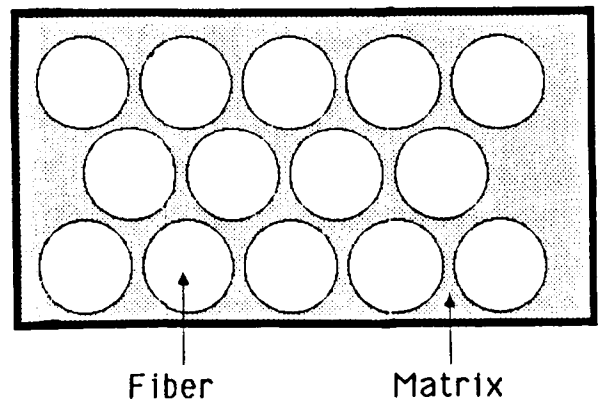


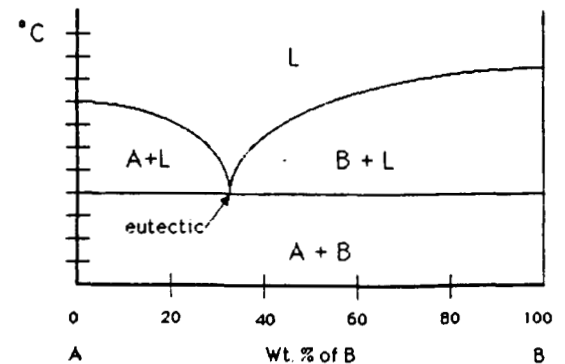
Figure 4

Composites of glass fibers in metal matrices have been investigated using aluminum as the matrix. Rolls Royce has shown (Arridge, 1964) that these composites can be made. Clemson University will investigate metal matrix alloys of magnesium/aluminum and iron/titanium. The four metals are all present on the Moon. The iron/titanium alloy is the most desirable because both metals are by-products of a process which reduces ilmenite (iron-titanium oxide) to produce oxygen.

Both magnesium/aluminum and iron/titanium alloys are used because eutectic points of each system occur at useable compositions (American Society for Metals, 1973). A eutectic point (Figure 5) occurs when the two end members of a system are mixed together at a certain ratio, producing an alloy with a minimum melting point. The magnesium/aluminum system has two eutectics: one at a weight percent of 68% Al and the other at 37.7% Al. The melting point of the first

is 451° C and that of the latter is 437° C. On the other hand the iron/titanium system has only one eutectic point which occurs at 67% Ti and which melts at 1068° C.

## Simple Binary Phase Diagram



Weight % A/B	°C
Mg/Al	
Mg 38 Al 62	@ 451
Mg 66 Al 34	@ 437
Ti/Fe	
Ti 65 Fe 35	@ 1068

Figure 5

This summer the Clemson group will first attempt to produce a composite utilizing ordered and/or randomly oriented bottle glass fibers in a magnesium/aluminum matrix. After successfully producing a composite of these materials, the Clemson team will investigate a composite incorporating glass fibers from simulated lunar regolith in a magnesium/aluminum matrix, and also the same fibers in an iron/titanium matrix.

#### GEOLOGY AND SITE SELECTION

People who choose a site for a lunar plant often use such criteria as topography or fuel economy (for getting into and out of orbit). This site was chosen based on raw materials availability. Since processing lunar soil or rocks could be energy-intensive, minimizing the raw material processing is important.

An overview of lunar geology is very simple. There are essentially two types of region on the Moon: maria and highlands. The maria, or lunar seas, are generally the dark areas. They are younger, fairly level lava flows that fill earlier impact basins. Basalt is the dominant rock type, and its composition varies widely. Pyroxene and feldspar (anorthite) are the dominant minerals, with significant amounts of olivine and ilmenite. The lunar highlands, on the other hand, are old pieces of original crust that have not been covered with lava. They are mostly anorthite and consequently are very light in color. Since they are so old, the highlands are saturated with craters. An

important fact to note is that the Moon's plagioclase feldspar is mostly (>95%) anorthite, which is the calcium end member. Sodium is rare on the Moon because most of it left with other volatiles (Taylor, 1982).

Regolith is the name for the lunar equivalent of soil. Meteoritic bombardment has broken, crushed, and mixed the upper layer of crust to form a fine, powdery soil. Regolith in the maria averages only one to five meters thick, while it averages ten to fifteen or even twenty meters thick in the highlands. This discrepancy is due to the difference in ages; the mare lavas flowed after most of the heavy meteoritic bombardment, thereby escaping most of the impacts. Highlands regolith is also more homogeneous than mare regolith because the crust (that is, the source material) is also more homogeneous, and has been mixed more (Taylor, 1982).

Many papers have suggested using basalt as a source material, or adding ingredients imported from Earth. This paper seeks to present a batch which does not rely on costly imported ingredients, and to show that basalt is not a good feedstock. This design team chose the Apollo 16 regolith as a raw material for the glass fibers for several reasons that are apparent from a knowledge of lunar geology. These reasons are: composition, particle size distribution, and abundance. Another important factor is that last year's Clemson team pulled fibers from synthetic material of this composition.

The Apollo 16 regolith is 75-90 weight percent anorthite;

another name for this material is anorthosite (McKay and Williams, 1979). As discussed earlier in this report, anorthite-rich material is superior to basalt as a glass-former because it is harder to crystallize. Referring to Table 2, it is also evident that this soil has less iron and titanium than other lunar soils. As stated previously, these elements induce nucleation, which reduces the strength of the glass. Table 3 shows, in addition, that this soil is very homogeneous. It only varies in oxide content about 3.8% over the 12 kilometer traverse over which samples were taken. No other lunar soil sampled during the Apollo missions approaches this homogeneity.

TABLE 2  
AVERAGE COMPOSITION OF APOLLO SOILS (WEIGHT %)

Oxide	11	12	14	15	16	17
SiO <sub>2</sub>	42.0	46.4	47.9	46.6	44.9	40.4
Al <sub>2</sub> O <sub>3</sub>	13.9	13.5	17.6	17.2	26.7	12.1
CaO	12.0	10.5	11.2	11.6	15.6	10.8
MgO	7.9	9.7	9.2	10.5	6.0	10.7
FeO	15.7	15.5	10.4	11.6	5.5	17.1
TiO <sub>2</sub>	7.5	2.7	1.7	1.4	0.6	8.3

After Rose, 1973

TABLE 3  
OXIDE CONTENT EXTREMES IN APOLLO 16 SOILS (WEIGHT %)

Oxide	Least	Most	Variation
SiO <sub>2</sub>	44.7	45.4	0.7
Al <sub>2</sub> O <sub>3</sub>	26.2	29.0	3.8
CaO	15.3	16.5	1.2
MgO	4.2	6.4	2.2
FeO	4.1	6.1	2.0
TiO <sub>2</sub>	0.4	0.7	0.3

After Rose, 1973

Apollo 16 regolith has a desirable particle size distribution. 95 weight percent of the particles are smaller than one centimeter in diameter, and 80 weight percent are smaller than 250 microns in diameter. It is easier and more desirable to melt small particles because the batch is more homogeneous at the outset. Moreover, no energy-intensive mining or crushing of solid rock is needed. Screening can efficiently produce a small-grained batch, and most of the soil by weight would be used.

Finally, highlands regolith is much thicker than mare regolith (Taylor, 1982). Since the source material is thicker per unit area, the transport system does not have to range as far. A deeper regolith also restricts the mining to a smaller surface area.



## LUNAR FIBERGLASS PLANT

Figure 6 is a flow chart of the lunar fiberglass production process. Figure 7 is a schematic of the entire plant. This section will examine each of the processing steps and components in detail. By referring to Figures 6 and 7, readers can see how each step or piece fits into the overall picture.

The first step is to mine the raw material. Several other schools, such as Georgia Institute of Technology, have

explored this area. The Clemson group assumed that some mining process involving scraping and/or scooping will be available.

After the regolith is mined, it must be transported to the plant. Several students investigated a cable car system which would transport the lunar soil (see Appendix A). Briefly, the system consists of a single cable with ore cars. The carriers will have weighing and position sensors built in. Regolith will be automatically transported from the mining site to the plant.

When the soil arrives at the plant, it will be preprocessed before melting (Figure 8). A screen or series of screens will

## Fiberglass Production Flow Chart

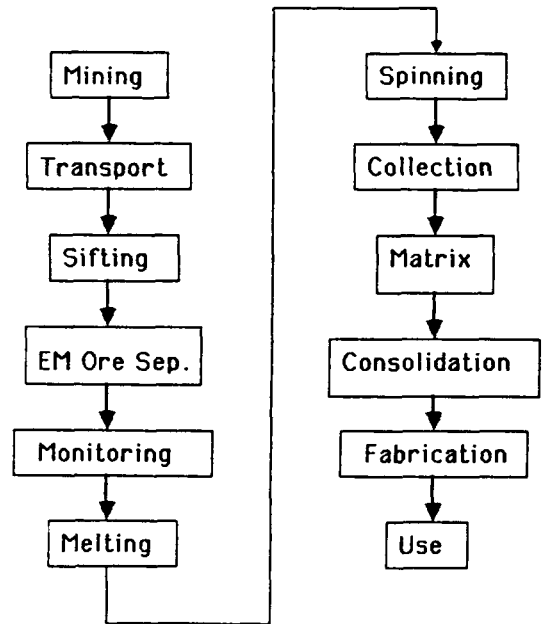
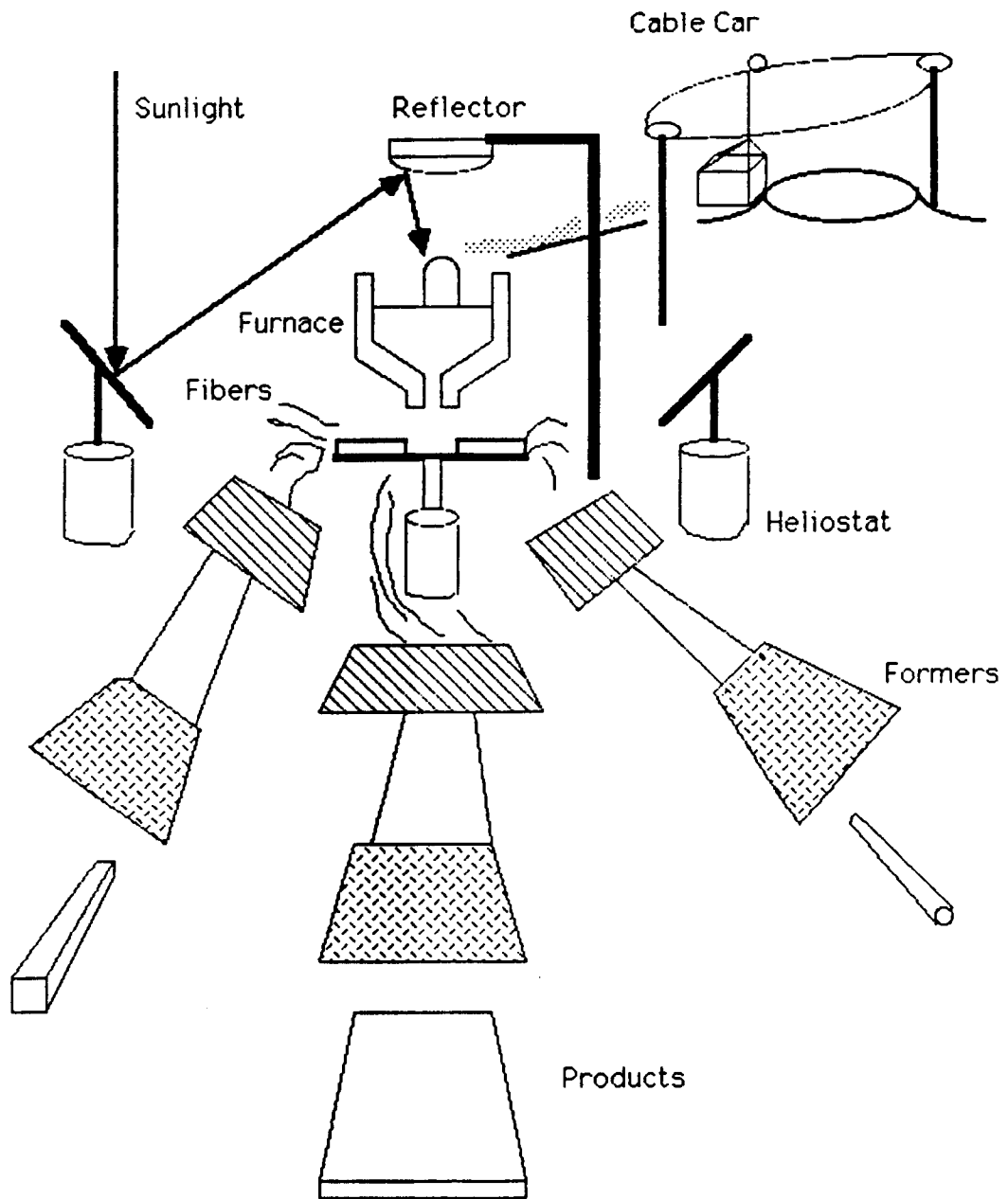


Figure 6

Figure 7

# Lunar Fiberglass Plant



## Preprocessing

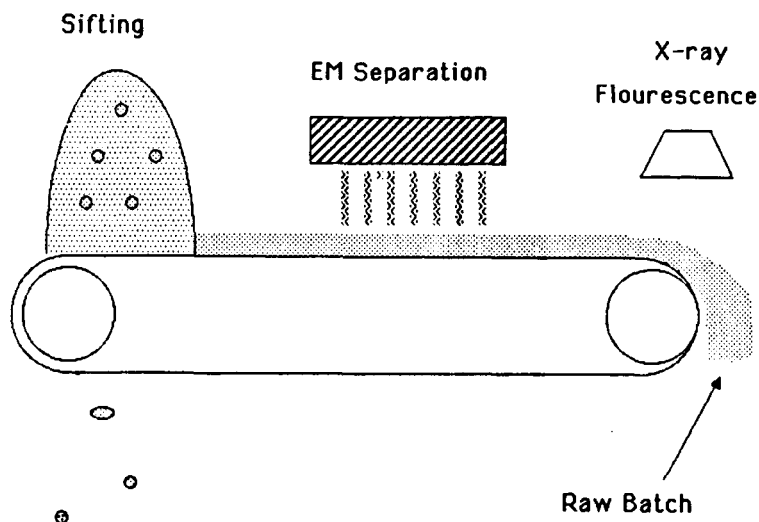


Figure 8

sort out larger fragments. Some of the iron may be removed via electromagnetic ore separation since iron and anorthite differ greatly in magnetic susceptibility. Finally, X-ray fluorescence of the batch will insure

that raw material of

roughly the correct composition arrives at the furnace.

The furnace is a hybrid unit, relying on both solar and electric power. This obviously means that the plant will only operate at peak capacity during the daylight hours. Figure 9 is a rough drawing of the furnace optics. A Cassegrainian setup with many heliostats as a primary mirror gives several desirable features. The heliostats are individually steerable, thus providing very fine control of the power input. There are no very large mirrors or structures. Also light enters the furnace from above. This fairly conventional setup lets us use a cylindrical furnace with a reservoir of molten glass and an exit hole in the bottom. See Appendix B for information on mirror numbers and sizing.

Figure 10 is a detailed drawing of the furnace. This design is a combination and modification of two Earth-based designs: the American Gas Institute furnace and the Pochet furnace (see Appendix C). The American Gas Institute furnace drops raw batch onto a hot knob at a temperature a few hundred degrees Celsius above the melting point, a very fluid melt flows down into the bottom of the furnace. The Pochet furnace is essentially a funnel with vertical electrodes in the bottom, around the bushing. Raw batch is added from the top and melts into the liquid glass. In Clemson's furnace a carbon-carbon composite refractory wall forms a cylinder with a funnel-shaped bottom. This cylinder will be about 0.5 meter in diameter and 1 meter high (see Appendix D

## Furnace Optics: Cassegrainian Setup

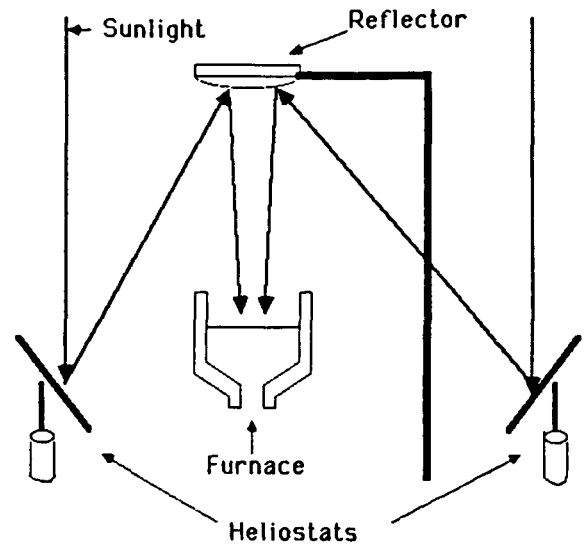


Figure 9

## Furnace

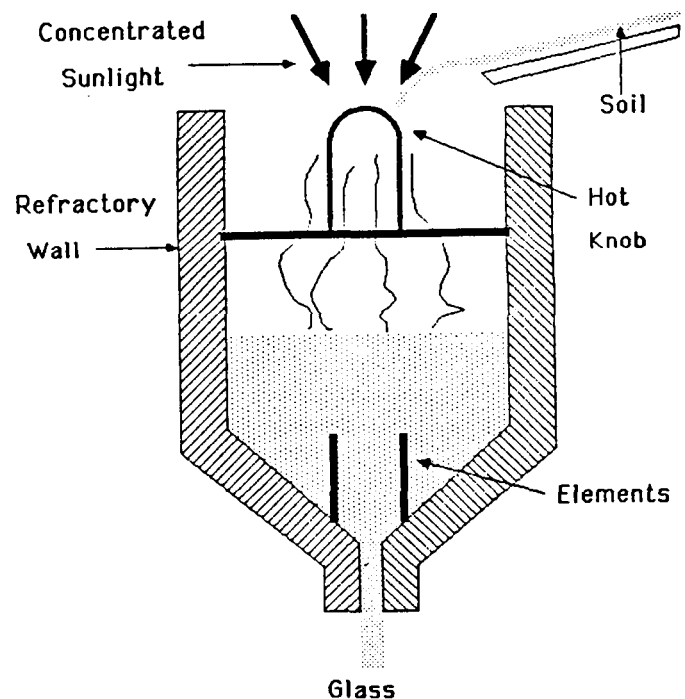


Figure 10

for furnace sizing). A molybdenum heat shield around the circumference of the furnace will reduce heat loss tremendously. A refractory knob is suspended by a set of crossed bars in the upper part of the furnace. This knob sits in the focal point of the furnace optics. Raw batch slides down a chute and falls onto the knob. The soil melts rapidly and falls into the molten glass reservoir. Electric heating elements made of molybdenum at the bottom of the tank provide fine temperature control of the glass stream. This furnace design is capable of operating at temperatures in excess of 2000° C.

Figure 11 shows the spinnerette, which turns the molten glass into glass fibers. Figure 12 is an oblique view. The spinnerette itself is a double-walled basket made of machined graphite. A current industrial version of this disk is about 18 inches in diameter and spins at about 2500 rpm.

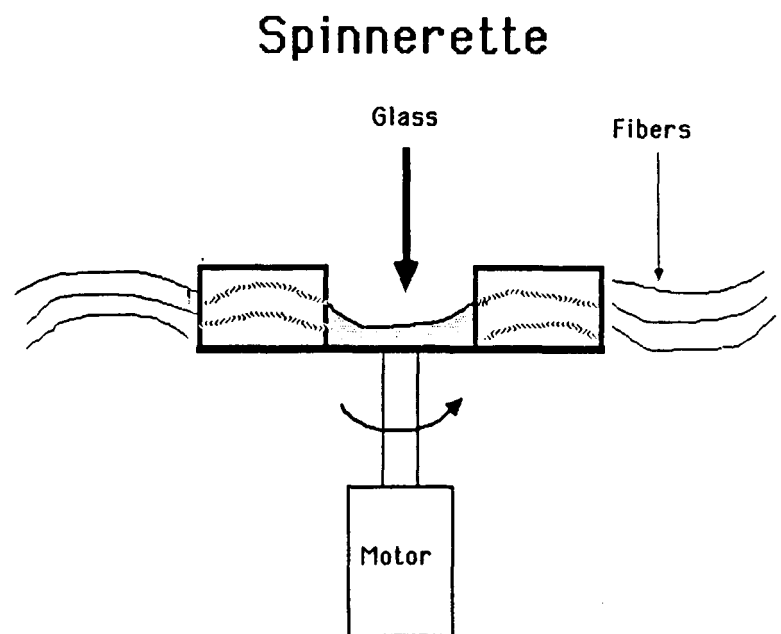


Figure 11

This rotation provides a centrifugal acceleration of roughly 1600 g's at the outer surface. Holes in the inner surface distribute glass streams to the outer surface. Fine holes in the outer surface force the glass into very fine, discontinuous

fibers. These fibers fly away from the disk in an arc. The entire process looks and behaves very much like a cotton candy machine.

The collection and coating process poses more problems than most of the other plant components. Figure 13 is Clemson's proposed solution. Double sets of wringer rollers are placed horizontally around the perimeter of the disk at a suitable distance. Fibers fly into the rollers, which are coated to prevent adhesion of the fibers to the rollers, and are compressed into a fibrous mat. Metal is added to this mat in

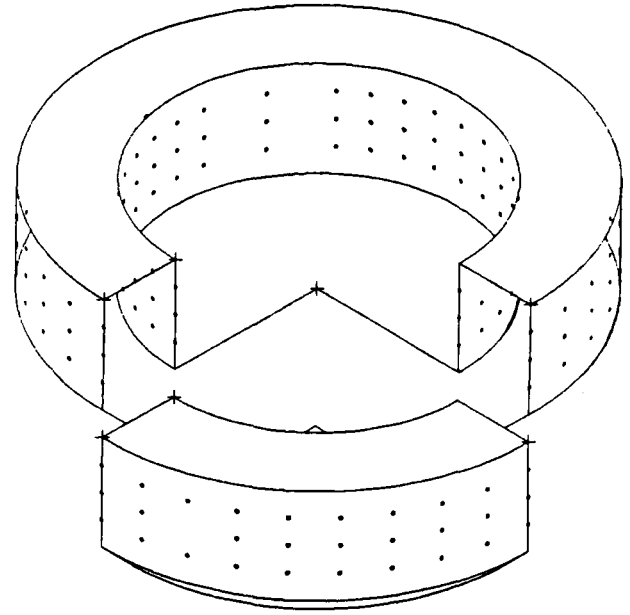


Figure 12

between the roller sets. The final set of rollers compresses and consolidates the product into a thin sheet of metal-matrix

fiberglass. The rollers may have to be heated to consolidate the

## Collection/Coating

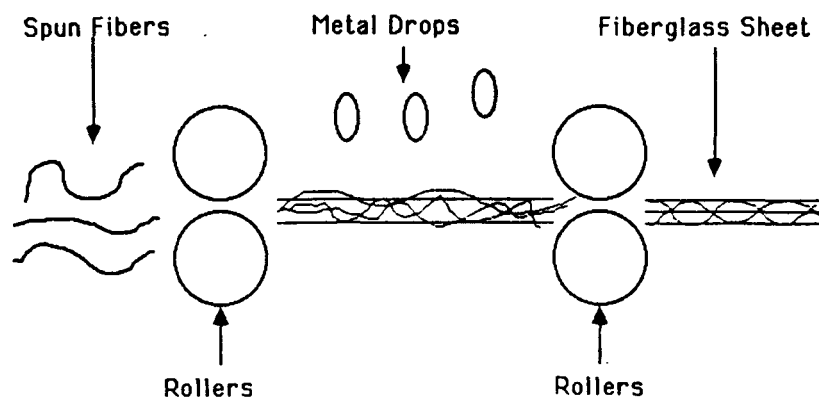


Figure 13

material properly. The glass and metal should stick to themselves and to each other fairly well; they will have a high surface energy in vacuum because there

will be no atmospheric gases or water vapor to contaminate the surface.

## End Products

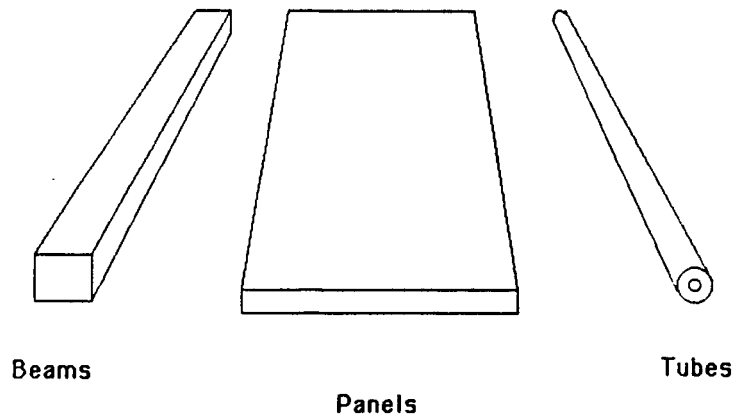


Figure 14

Lunar base construction will demand more than thin fiberglass sheets. Figure 14 shows some of the stock end products that the base will require. The roller setup is quite versatile, since each roller set can produce a different product. Beams can be made

by folding fiberglass sheets back and forth accordion-style and pressing them together. Panels similar to plywood will result from pressing several sheets of fiberglass together. Tubes and rods can be made by rolling a fiberglass sheet until the desired thickness is obtained. As the plant matures, more advanced shapes may be developed.

### SUMMER APPARATUS

The 1987 summer experimental apparatus (Figure 15) still utilizes the textile process as did last year's setup; however, some changes were made. The vapor generator which was to coat the fibers has been replaced with a liquid metal melt pot. The melt pot will form a drop of metal held in place by surface tension

## Setup for Making Samples

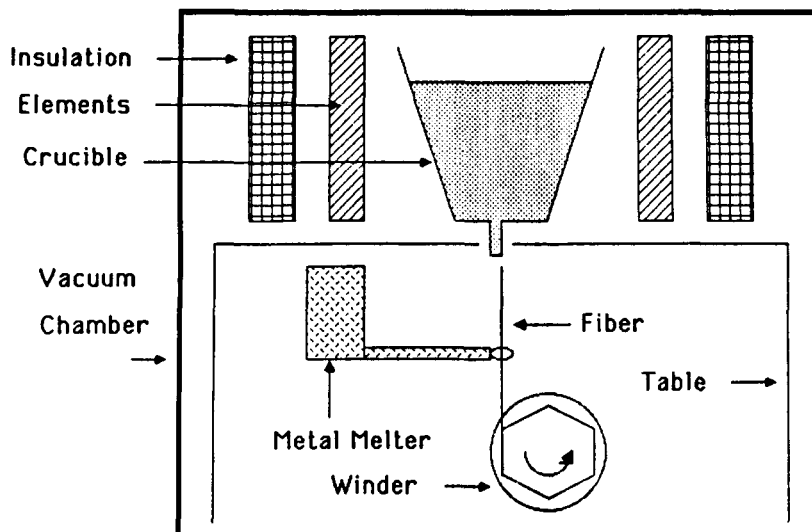


Figure 15

(Arridge, 1964). The fiber will be coated as it passes through the droplet.

The glass melt furnace has been redesigned to withstand temperatures in excess of 1600° C. Three layers of insulation are used instead of

one. The inner wall is made of 1.5-inch-thick 1600° C rated fiberboard; next is a buffer zone of 1/4-inch of Kaowool™ blanket, and the outside wall is 1/2-inch-thick 1400° C rated fiberboard.

The system still uses a 6.25-inch diameter take-up reel capable of safely turning at 425 rpm. A new stand-alone microprocessor-based programmable controller for the translation motor was designed; it will be built at Johnson Space Center. A digital optical tachometer that resolves to the nearest rpm, updates every second, and has a bus suitable for adding closed-loop speed control was also built. The furnace, in addition, has its own heavy-duty metered variac.

An independent metal-melting furnace was built at JSC. Metal will be melted in crucibles in this furnace. Several techniques for making composites will be studied: forming a



randomly-oriented composite by mixing short fibers into liquid metal, forming a unidirectional composite by wicking metal up through a fiber bundle, and generating an ordered composite by pouring matrix material over oriented fibers.

## SUMMER WORK

### Experiments

- 1) Examine lunar glass compositions that follow the trend of soil samples 60501 and 61221 and glass sample 67975.
- 2) Produce a metal-matrix composite of bottle glass fibers in a Mg/Al alloy matrix
- 3) Produce a metal-matrix composite of lunar glass fibers in a Mg/Al alloy matrix
- 4) Produce a metal-matrix composite of lunar glass fibers in an Fe/Ti alloy matrix
- 5) Process and melt glass in a vacuum
- 6) Produce a composite in vacuum

### Construction

- 1) Build a temperature control center for the glass melting furnace
- 2) Build a glass droplet catcher for use in the vacuum chamber
- 3) Build the microprocessor-based stepper motor controller

## CONCLUSION AND RECOMMENDATIONS

This report presents a design for a lunar plant that makes fiberglass from Apollo 16 regolith. The Clemson University design team intends for this plant to help build the infrastructure for a largely self-supporting lunar base. The subsystems need more detailed work, and some experimental work is needed. The science of lunar glass compositions matrix metals, and their behavior and interactions under lunar conditions need to be studied in the laboratory. This information is needed in order that an optimum process and material be fully designed.

## APPENDIX A: AERIAL ROPEWAY TRANSPORTATION SYSTEM\*

\*Note: This text is taken verbatim from a Transportation Committee report written by Birgit Loescher.

### Advantages

There are many advantages which favor an aerial ropeway as a lunar raw material transport system. According to Schneigert (1966), construction time for an aerial ropeway is shorter than for railroads or roads, the unloading and loading is suited toward full automation, steep gradients can be surmounted, and the service life can exceed 10 to 15 years. The Trenton Iron Company (1896) lists other advantages as being "free from service traffic", having low operation costs, and the ability to load and unload at the exact spots needed, thus eliminating rehandling. Furthermore, the aerial ropeway has the main advantage of flexibility and adaptability for going into the craters and over the high hills on the lunar surface.

### Disadvantages

Several disadvantages of an aerial railway system include: fixed location of load-unload stations and rigidity of the route (Schneigert, 1966). In addition, the implementation of this system assumes that enough material can be mined from an area to justify the set-up of a system. Although the system can be made transportable (Schneigert, 1966), the cost of each move in manpower and energy might prove to be a major limiting factor. However, despite these disadvantages, the aerial railway still

provides a viable solution to the problem of raw material transportation.

### Components

Industrial Ropeways were first patented in 1856 (Schneigert, 1966). Although much has changed in the way of energy generation and motor drives since that time, the basic principles of ropeways have remained. A "car" travels along a ropeway which is circulating or fixed from a beginning "station" to an end "station". The component parts of an industrial ropeway (Figure 16) include the ropes, the cars, the trestles, the stations, and the driving and return gears (Schneigert, 1966).

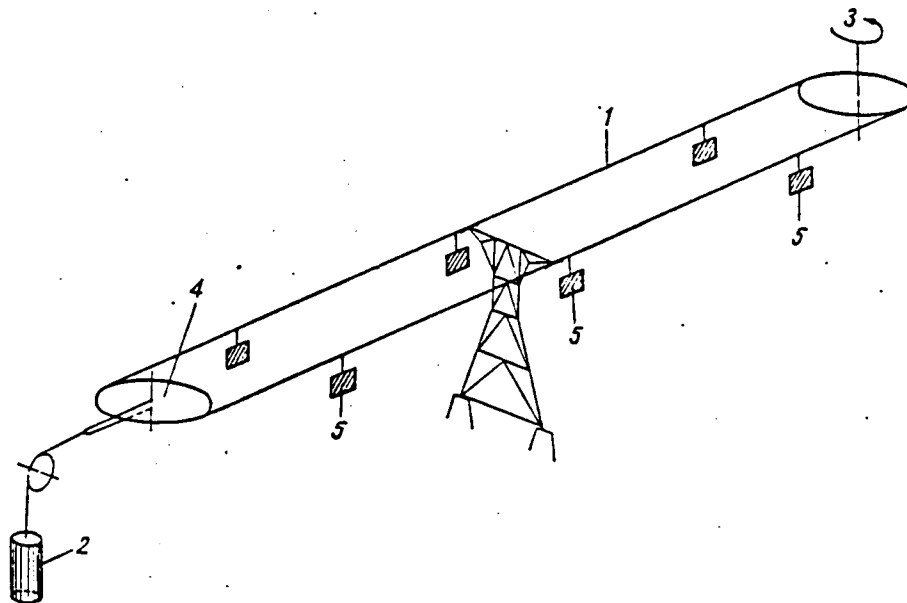


FIG. 19. Arrangement of a monocable ropeway.  
1 — carrying-hauling rope, 2 — tension weight, 3 — drive, 4 — return sheave, 5 — cars.

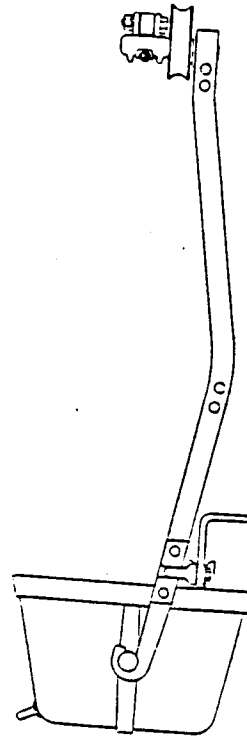
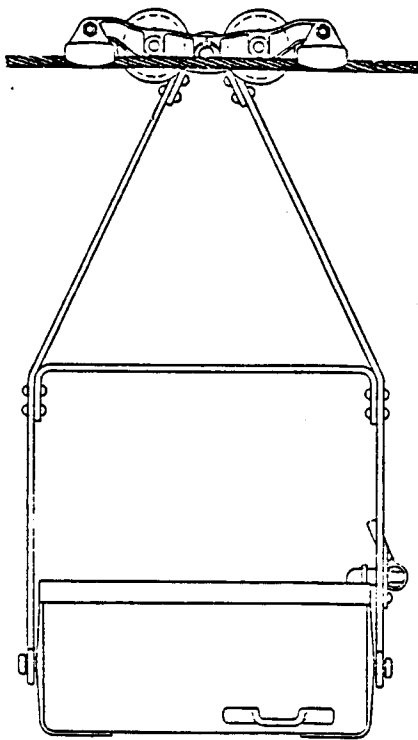
Figure 16

The ropes used in an aerial ropeway are made of steel wire for the purpose of carrying and hauling tension as well as signalling (Schneigert, 1966). A ropeway can be classified by the

number of ropes it uses. A monocable ropeway only has a single rope which carries and pulls a car. A bicable ropeway has two ropes: one to carry the car and the other to pull the car. The Trenton Iron Company (1896) recommends a single line for "short lines and light service." It can carry loads up to 150-200 tons per hour (Schneigert, 1966). In applying this to a lunar transportation system, a monocable system should be employed initially as the amount of raw material projected is of a small quantity. This then can be made transportable to relocate to another site or can also be upgraded into a bicable system if an increase in needed load should occur.

The cars (Figure 17) consist of a lock-unlock device, hangar, and carrier (Schneigert, 1966). Cars can be made to tip their contents automatically or unlock at a station. Loading can also be similarly accomplished. To solve the problem of moving metal parts "sticking" in a vacuum, a self-lubricating system should be incorporated into the carriage.

Trestles support the rope at points in between stations. The number and height of the trestles depend on the ground profile over which the rope travels (Schneigert, 1966). Trestles can be made of steel, reinforced concrete, or wood. Considering the need for limiting the weight of building materials transported to the Moon, a lightweight metal frame system that can be assembled on the lunar surface would be the most economical system. However, problems may be encountered in developing a stable concrete foundation from lunar materials for the trestles.



The stations house the driving and return gears for the ropeway. They terminate each ropeway section at each end (Schneigert, 1966). Electricity, generators, and engines act as sources of supply of the needed power. The speeds necessary to load -- unload without

stopping the cable are usually 1 to 3 m/s (Schneigert, 1966). The amount of material to be transported will be the determining factor in the amount of power needed.

Loading and unloading can be accomplished by unlocking and locking cars at either or both ends. Automatic measuring feeders which use conveyor belts can unload without taking the car off the line (Schneigert, 1966). Materials can be stockpiled near the unloading station (located as close to the furnace as feasible).

The use of an aerial ropeway transportation system to move raw materials from mine to factory on the lunar surface appears to be a workable solution. Its design has been used extensively and successfully in industry. It is hoped that this transport system will not only aid in the success of the facility but also aid in the facility's growth.

## APPENDIX B: MIRROR OPERATION AND SIZING

The total insolation falling on the primary furnace mirrors is proportional to the cosine of the sun's angle from the zenith. If the minimum power that we want available is 1/2 of that peak input (corresponding to 1/2 of the mirrors totally illuminated), then we have an operations "window" 120 degrees wide:

$$\arccos 0.5 = 60^\circ$$

$$\begin{array}{l} 60^\circ \text{ increase of sun angle on one side} \\ + 60^\circ \text{ decrease of sun angle on opposite side} \\ \hline 120^\circ \text{ total available for operating furnace} \end{array}$$

This span is 1/3 of a lunar day, or 9.1 Earth days. Of course, operation outside this window is possible. The decreasing solar energy is still useful heat. The same throughput may be maintained with increased electricity useage, or the same level of power useage will result in decreased production.

The primary mirror sizing equation depends on these variables:

F - furnace input power (W)

N - number of mirrors

P - insolation (W/m<sup>2</sup>)

emp - mirror reflectivity for a primary heliostat

ems - mirror reflectivity for the subreflector

C - concentration ratio of subreflector

The concentration ratio of the subreflector is the ratio of the subreflector area to the focussed spot area:

$$C = \frac{A}{S} ,$$

where

A = area of subreflector (m<sup>2</sup>)

S = area of spot (m<sup>2</sup>)

We will use the following values:

P = 1380 W/m<sup>2</sup> (given)

emp = 0.95 (assumed)

ems = 0.95 (assumed)

S = 0.01767 m<sup>2</sup> (for a 15-cm diameter hot spot)

The design equation is as follows:

$$F = \frac{N}{2} * P * emp * ems * \frac{A}{S} ,$$

which reduces to:

$$F = 35,239 * A * N$$

The final selection of A and N depends on such factors as the convenient size of a heliostat and how much power the furnace will require. The latter is greatly dependent of the emissivity and reflectivity of the raw batch. These concerns have not been fully addressed yet.



## APPENDIX C: PARENT FURNACES

### Pouchet Furnace

- 1 - Raw Batch
- 2 - Refractory Wall
- 3 - Molten Glass
- 4 - Electrodes

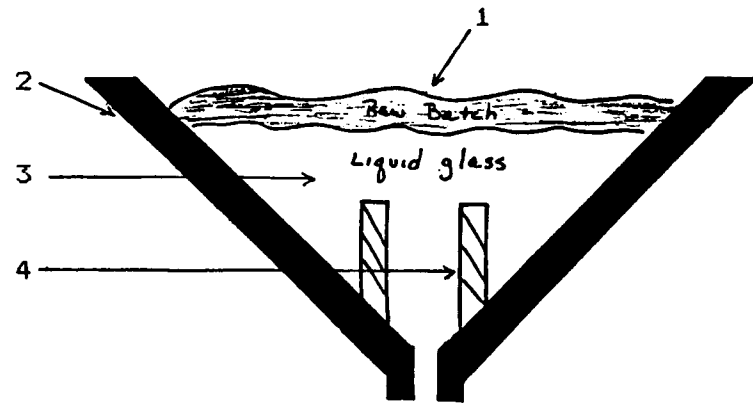


Figure 18 - Pochet Furnace

### American Gas Institute Furnace

- 1 - Batch Feed
- 2 - Gas Flames
- 3 - Hot Knob
- 4 - Molten Glass
- 5 - Refractory Wall

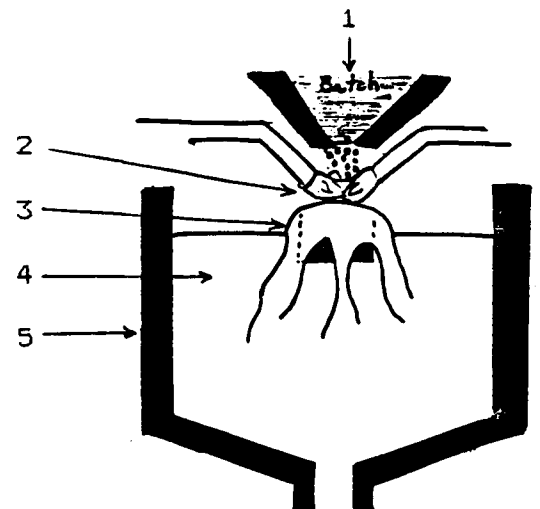


Figure 19 - American Gas Institute Furnace

## APPENDIX D: LUNAR FURNACE SIZING

The design parameters which yield furnace dimensions for a given production rate can be calculated from the following equation (variables reference Figure 20):

$$\text{flow rate} = \frac{r^4 * h}{l * n} * D * g$$

where

r = radius of the nozzle

h = height of the glass above the nozzle

l = length of the parallel section of the nozzle

n = viscosity of the glass

D = density of the glass

g = acceleration due to gravity

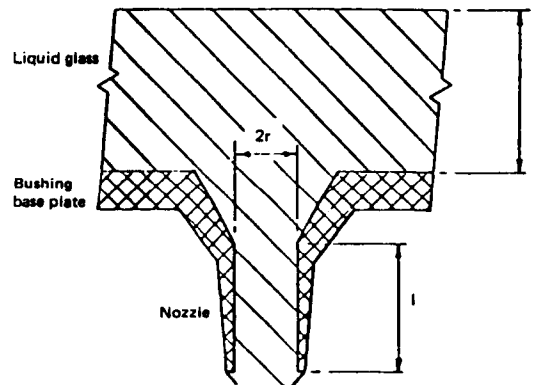


Figure 20 - Glass Nozzle Parameters (Doyle, 1979)

Observing that  $g$  is in the denominator, it can be seen that a flow rate on Earth would be six times greater than one calculated for the Moon.

## REFERENCES

- American Steel & Wire Company. Aerial Wire Rope Tramways (New Jersey: American Steel & Wire Company, 1935), pp. 3-50.
- Arridge, R. G. C., Baker, A. A., and Cratchley, D. "Metal coated fibres and fibre reinforced metals", Journal of Scientific Instrumentation, Vol. 41, 1964, pp. 259-261.
- Doyle, P. J. Glass Making Today. Portcullis Press Ltd., Surrey, England (1979), 343 pp.
- Klein, L. C., and Uhlmann, D. R. "Crystallization Behavior of Anorthite," Journal of Geophysical Research, Vol. 79, No. 32, Nov. 10, 1974, pp. 4869-4874.
- McKay, David S., and Williams, Richard J. "A Geologic Assessment of Potential Lunar Ores", Space Resources and Space Settlements, NASA SP-428 (1979), pp. 243-255.
- Ridley, W. I. et al. "Compositions in Apollo 16 soil 60501 and 61221", Proceedings of the Fourth Lunar Science Conference, Vol. 1, pp. 309-321.
- Rose, H. J. et al. "Compositional Data for Twenty-two Apollo 16 Samples", Proceedings of the Fourth Lunar Science Conference, Geochimica et Cosmochimica Acta. Supplement 4, Volume 2, 1973, pp. 1149-1158.
- Schneigert, Zbigniew. Aerial Ropeway and Funicular Railways (Poland: Pergamon Press, 1966), pp. 4-317.
- Taylor, Stuart Ross. Planetary Science: A Lunar Perspective. Lunar and Planetary Institute, Houston (1982), 473 pp.
- Trenton Iron Company. Wire Rope Transportation (Trenton, N. J.: Cooper, Hewitt & Company, 1896), pp. 5-40.
- Uhlmann, D. R., Klein, L. C., and Handwerker, C. A. "Crystallization Kinetics, Viscous Flow, and Thermal History of Lunar Breccia 67975," Proceedings of the 8th Lunar Science Conference, pp. 2067-2078.